Fluid Phase Equilibria 292 (2010) 110–116

Contents lists available at ScienceDirect

Fluid Phase Equilibria

journal homepage: www.elsevier.com/locate/fluid

Shift of the azeotropic point of binary Lennard–Jones mixtures confined in a slit-like pore

Ying-Feng Li, Yang-Xin Yu*, Yuan-Xiang Zheng, Ji-Ding Li

Department of Chemical Engineering, Tsinghua University, Beijing 100084, PR China

ARTICLE INFO

Article history:
Received 22 November 2009
Received in revised form 1 February 2010
Accepted 11 February 2010
Available online 18 February 2010

Keywords:
Azeotrope
Vapor–liquid equilibria
Lennard–Jones mixture
Confinement
Monte Carlo simulation

ABSTRACT

The Gibbs ensemble Monte Carlo simulation is used to investigate the vapor–liquid phase behavior of a binary Lennard–Jones mixture confined in a slit-like pore at reduced temperature $T^* = 1.0$. Our simulation program is tested by comparing the simulated phase diagram with the previous simulation results from various methods. Then phase diagrams of a binary asymmetric Lennard–Jones mixture confined in the slit-like pores are investigated by varying the pore width and fluid–pore wall interaction. The asymmetric system studied exhibits azeotropic behavior. The pore walls are symmetric but selective to the two components. The simulated results indicate that both the pore width and interactions between fluid and the pore wall have significant influence on the vapor–liquid phase diagram for the binary Lennard–Jones mixture. When the interaction energy parameter between component 1 and the pore wall is fixed, the azeotropic point is shifted from the bulk azeotropic composition to component 2-rich side of the phase diagram as the interaction strength between component 2 and the pore wall is increased. In the meantime, both the azeotropic pressure and the relative volatility increase significantly. As the pore becomes narrower, it is found that the azeotropic pressure increases significantly while the azeotropic composition remains almost unchanged. The phase selectivity decreases as the pore becomes narrower in the whole range of composition. All the simulated results suggest that the azeotropic point of a binary mixture can be shifted or even be removed by the confinement and the relative volatility for vapor–liquid equilibria can be changed greatly by changing the pore width or fluid–pore wall interactions.

1. Introduction

Since confined fluids are involved in many physical and chemical processes such as membrane separation process and chemical reaction in micro-reactor, understanding their thermodynamic and kinetic properties is of great importance from both theoretical and application points of view [1]. The vapor–liquid phase diagram in confined space is dramatically different from the corresponding bulk one due to the interplay of the fluid–fluid and fluid–wall interactions [2]. For example, the vapor–liquid critical temperature in the confinement is lower than that in bulk, as can be seen from experiments [3], molecular simulations [4] and density functional theories [5]. The capillary condensation, layer transition and adsorption behavior of simple fluids in slit-like or cylindrical pores [6] have been widely investigated using grand canonical Monte Carlo (GCMC) simulations [7–11] and density functional theories [12,13].

In the molecular simulations, several powerful methods are available for the study of the phase diagram. These methods include the Gibbs ensemble Monte Carlo (GEMC) [14], semigrand Monte Carlo (SGMC) [15], Gibbs–Duhem integration [16] and transition-matrix Monte Carlo (TMMC) [17] simulations. Among these methods, the GEMC simulation has always remained popular both because of its physical, intuitive nature and its perfect performance on the vapor–liquid and liquid–liquid equilibrium prediction far from the critical point.

The GEMC method is a direct method for determining the coexisting phases. In this approach, the existing phases are simulated simultaneously in two separate boxes and the equilibrium is reached by particle displacements inside each simulation box, volume changes, and particle exchanges between the two simulation boxes. It has been widely used to simulate the phase diagram of various fluids in bulk case [18–20]. And it has also been extended to estimate the adsorption and phase diagram for pure fluids confined in narrow pores. For example, the GEMC method has been extended for the prediction of adsorption and capillary condensation of simple fluids in narrow cylindrical pores [21]. The liquid–liquid equilibria in the slit pores for a simple Lennard–Jones symmetric mixture have been reported by Kierlik et al. [22] and Gozdz et al. [23]. Sliwinska-Bartkowiak et al. [24] have investigated the liquid–liquid transition in cylindrical pores by the GEMC simulation and density functional theory. Kanda and

* Corresponding author. Tel.: +86 1062782558; fax: +86 1062770304.
E-mail address: yangxyu@mail.tsinghua.edu.cn (Y.-X. Yu).

0378-3812/$ – see front matter © 2010 Elsevier B.V. All rights reserved.
doi:10.1016/j.fluid.2010.02.008

Table 1
The values of potential parameters for binary Lennard–Jones mixtures.

Mixture	σ_{22}/σ_{11}	σ_{12}/σ_{11}	$\varepsilon_{22}/\varepsilon_{11}$	$\varepsilon_{12}/\varepsilon_{11}$
Symmetric	1.0	1.0	1.0	0.75
Asymmetric	1.15	1.075	1.0	0.75

Makino [25] have reported the liquid–liquid interface properties of the Lennard–Jones symmetric mixture in the slit pore. All above mentioned studies show that the effect of confinement is to lower the critical mixing temperature, and to reduce the range of immiscibility. When the fluid–wall attraction is greater for component 1 than for component 2, the liquid–liquid coexistence curve is shifted towards the 1-rich side of the diagram. However, we have not found any molecular simulation studies on the vapor–liquid phase diagram for fluid mixtures confined in pores by the GEMC method, or even other simulation technologies.

The separation of a homogeneous azeotropic mixture is a common task in the chemical industry. The traditional distillation is unsuitable for the separation of this kind of mixture and some new methods are still in demand. The knowledge of azeotropic behavior is also important when considering mixtures for their use as refrigerants [26]. A computational strategy and methods for the automated calculation of complete loci of homogeneous azeotropy of binary mixtures have been proposed based on the equation of state [27]. But the confinement effect on the azeotropic behavior of binary systems has not been understood. The objective of this work is a simulation analysis of the shift of the azeotropic point by the confinement. We systematically study the effect of the pore width and fluid–wall interaction on the vapor–liquid phase diagram for the confined Lennard–Jones mixture with an azeotropic point.

2. Model and simulation details

The Lennard–Jones 12–6 potential is a very important model for exploring the phase behavior of simple fluids. In this work, we consider the binary Lennard–Jones mixture confined in the slit-like pores. The interactions between each pair of particles are represented by a truncated Lennard–Jones potential, i.e.,

$$u_{ij}(r_{ij}) = \begin{cases} 4\varepsilon_{ij}\left[\left(\dfrac{\sigma_{ij}}{r_{ij}}\right)^{12} - \left(\dfrac{\sigma_{ij}}{r_{ij}}\right)^{6}\right] & r_{ij} < r_c \\ 0 & r_{ij} > r_c \end{cases} \quad (1)$$

where r_{ij} is the center-to-center distance between particles of types i and j, and σ_{ij} and ε_{ij} are, respectively, the size and energy parameters for the interaction potential. r_c in Eq. (1) is the cutoff distance. According to the convention, the smaller species is considered to be species 1 and its interaction parameters σ_{11} and ε_{11} are assigned as the units of length and energy, respectively. In this work, a binary symmetric and a binary asymmetric Lennard–Jones mixture, both exhibiting azeotropic behavior, are investigated. The potential parameters of the two binary systems studied are listed in Table 1.

The slit-like pore studied in this work is represented by two infinite parallel plates separated by a physical width H in the z direction. The pore walls are energetically homogeneous. The interaction between fluid and the pore wall is a function of the normal distance to the wall, and can be expressed by the Lennard–Jones (9–3) potential, i.e.,

$$v_{wi}(z) = \varepsilon_{wi}\left[\left(\frac{z_{oi}}{z}\right)^{9} - \left(\frac{z_{oi}}{z}\right)^{3}\right] \quad (2)$$

where $i = 1$ and 2, z is the perpendicular distance of the fluid particle i from the wall, ε_{wi} is the interaction energy parameter between fluid particle i and pore wall, and z_{oi} is the size parameter, which is set to be $0.5\sigma_{11}$ in this work. When a fluid particle is confined in the slit-like pore, the external potential $V_i^{\text{ext}}(z)$ ($i = 1, 2$) can be expressed as

$$V_i^{ext}(z) = v_{wi}(z) + v_{wi}(H - z) \qquad (i = 1, 2) \quad (3)$$

In the GEMC simulations, the vapor–liquid phase diagrams of the binary Lennard–Jones mixtures were determined in two simulation boxes: one corresponding to the liquid phase and the other corresponding to the vapor phase. We performed three types of Monte Carlo moves, displacements of a randomly selected molecule inside each simulation box, volume changes of the two boxes by equal and opposite amounts, and the particle exchanges between the two simulation boxes.

For the bulk simulation, 2000 particles were used and three-dimensional periodic boundary conditions were adopted. The potential cutoff distance was set to be $5.0\sigma_{11}$. The typical calculation consisted of 9×10^4 Monte Carlo cycles in which the last 4×10^4 Monte Carlo cycles were used to sample and average. Each Monte Carlo cycle involved one translation move for each particle, one volume change attempt, and 100–200 molecule transfer attempt. For the case of slit-like pores, the simulation parameters were the same as those in bulk case except that the periodic boundary conditions were only adopted in the x- and y-directions, and the potential cutoff distance was set to be $6\,\sigma_{11}$.

Although the pressure can be calculated in a standard way from the virial, it can be calculated directly in the molecular simulation by performing trial volume changes to compute $(\partial\beta A^E/\partial V)_{T,N}$, where $\beta = 1/k_BT$, k_B is the Boltzmann constant, T is the absolute temperature, A^E is the excess Helmholtz free energy, V is the volume, and N is the number of particles in the system. Following the work of Harismiadis et al. [28] and Vortler and Smith [29], we applied this approach to the calculation of the pressure in Gibbs ensemble simulations. The pressure was obtained by taking the limit $\Delta V \to 0$, i.e.,

$$\beta p = -\lim_{\Delta V \to 0} \frac{\ln\left\langle \exp(-\beta \Delta U)\right\rangle_0}{\Delta V} \quad (4)$$

where ΔU is the total potential energy change when the volume is changed by the trial volume change ΔV, $\langle\cdots\rangle_0$ denotes a canonical ensemble average over configurations of the reference systems. In practice, the pressure was determined by extrapolating the ratio in Eq. (4) to $\Delta V = 0$.

In all simulations, we adjusted the maximum possible displacement and maximum volume change to obtain an average acceptance of 50% for translation moves and volume changes. The number of particle transfer is adjusted to achieve about 1–2 accepted transfers per Monte Carlo cycle. A simulation run was divided into many blocks and each block covered about 10 Monte Carlo cycles. Firstly, the block average properties were calculated by accumulating and averaging the instantaneous properties over the Monte Carlo cycles within a block. Then the total average properties were obtained from the block average properties. At last, the estimated errors were obtained from the standard deviation of the block average properties. This block averaging technique has been successfully applied in the molecular simulation in the previous work [30].

3. Results and discussion

3.1. Validation of the GEMC simulation program

We have simulated the vapor–liquid equilibria for bulk binary symmetric Lennard–Jones mixture at reduce temperatures $T^* = 1.0$ and 1.15 to validate the GEMC simulation program. Here the reduced temperature T^* is defined as $T^* = k_BT/\varepsilon_{11}$. All the interac-

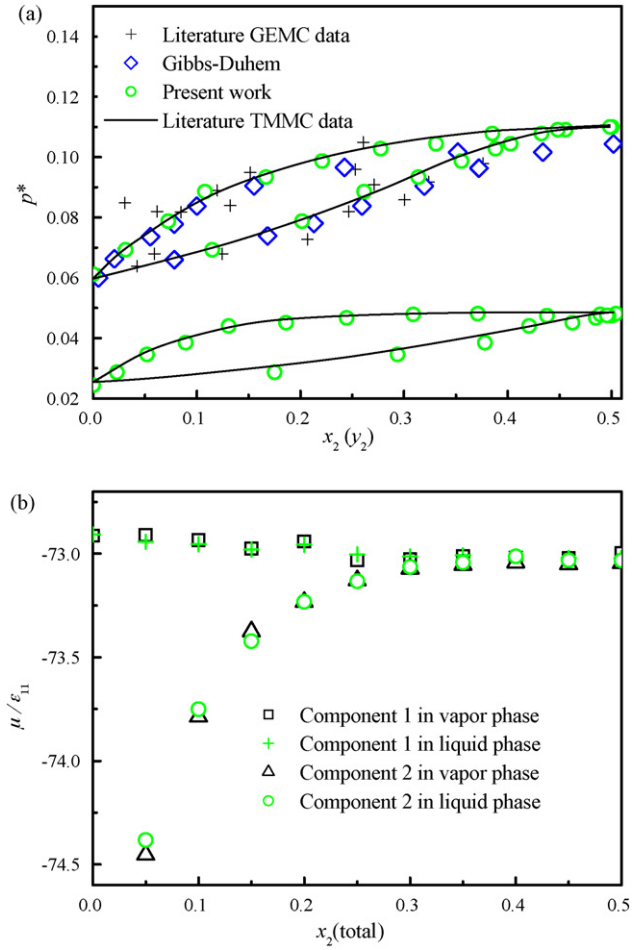

Fig. 1. (a) Vapor–liquid phase diagram in the pressure-composition plane for a binary symmetric Lennard–Jones mixture exhibiting azeotropic behavior at reduced temperatures T^* = 1.0 and 1.15. Circles are the results from the present GEMC simulation algorithm, and solid lines are the results from TMMC simulations [17]. GEMC simulation data (+) generated by Panagiotopoulos et al. [14], and Gibbs–Duhem integration data (◊) obtained by Mehta and Kofke [31] are also plotted in the figure for comparison. Only the left branch of phase diagram is given because it is symmetric. (b) Chemical potentials of the two components in vapor and liquid phases for the system in (a) at reduced temperature T^* = 1.0.

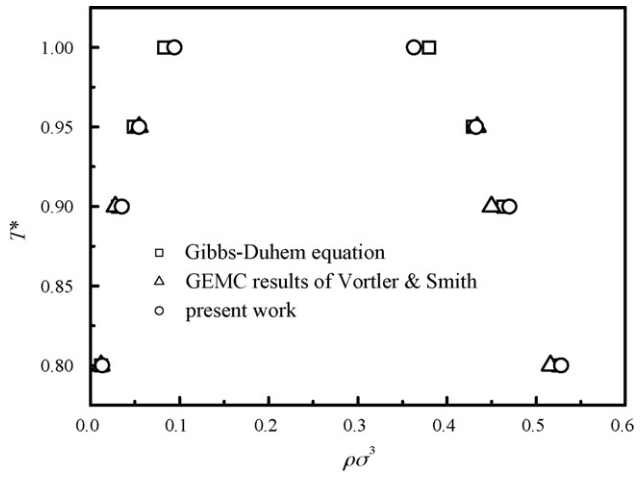

Fig. 2. Temperature-density vapor–liquid coexistence for the square-well fluid with parameter λ = 1.5 in a hard planar slit pore with width H/σ = 4.0. Squares, triangles and circles are the phase equilibrium data obtained by using smoothed chemical potentials in conjunction with the Gibbs–Duhem equation, from the GEMC simulations of Vortler and Smith [29], and from the present work, respectively.

tion parameters for the binary symmetric Lennard–Jones mixture can be found in Table 1, which give rise to an equimolar azeotrope at moderate temperature. The pressure-composition projection of the vapor–liquid phase diagram for this symmetric mixture is plotted in Fig. 1(a). For comparison, the simulated results from previous studies using the GEMC [14], TMMC [17] and Gibbs–Duhem integration [31] are also included in Fig. 1(a). Because the vapor–liquid phase diagram for this mixture is symmetric, only left branch of the phase diagram is shown in Fig. 1(a). In our simulation we have used a cutoff distance $r_c = 5\sigma_{11}$ with a long-range correction. We have increased ten times the run length for one case at higher temperature and one at lower temperature, and no effect on the results is found. This shows that our simulation run length is long enough. The agreement between our simulations and the literature TMMC results is very good. The azeotropic pressures estimated from our simulations are 0.110 at T^* = 1.15 and 0.0502 at T^* = 1.0, which show very good agreement with the literature azeotropic pressures 0.110 and 0.0484.

To make sure that equilibrium have been achieved before any property averages can be calculated, it is customary to monitor the approximate equality of the vapor–liquid equilibria of a binary mixture. We report the chemical potentials μ of the two components in both phases for the symmetric mixture in Fig. 1(b) at reduced temperature T^* = 1.0. The simulated chemical potentials are computed with a long-range correction. From the figure we find that chemical potentials of each component in the vapor and liquid phases are very close to each other. The maximum differences in chemical potentials between the two phases for components 1 and 2 are $0.031\varepsilon_{11}$ and $0.070\varepsilon_{11}$, respectively. These results indicate that the equilibrium conditions have been reached in the sample and average stage of the molecular simulations. According to the results shown in Fig. 1 we can conclude that our GEMC simulation program is accurate and suitable for investigating the vapor–liquid phase coexisting properties of binary Lennard–Jones mixture.

To validate our GEMC simulation program for confined fluids, we have computed the vapor–liquid equilibria for square-well fluid in the hard slit-like pore. The results are compared with literature data in Fig. 2. Here the width of the hard slit pore is H/σ = 4.0 and the range parameter for the square-well fluid is λ = 1.5. From Fig. 2 we can see that our simulation data are in good agreement with those from the GEMC simulations of Vortler and Smith, and those obtained by using the smoothed chemical potentials from the simulations in conjunction with the Gibbs–Duhem equation. These results indicate that our GEMC simulation program is also applicable to the study of phase diagram for the confined fluids.

3.2. *Asymmetric binary mixture confined in slit-like pores*

We have used the GEMC simulations to investigate the vapor–liquid phase diagram for the binary asymmetric Lennard–Jones mixture in bulk and confined in slit-like pores. In all the simulations for the asymmetric binary Lennard–Jones mixture, the reduced temperature is set to be T^* = 1.0, and the cutoff distance for the Lennard–Jones potential is enlarged to be $r_c = 6\sigma_{11}$ for more accuracy. The potential parameters for the binary asymmetric Lennard–Jones mixture can be found in Table 1. Fig. 3 depicts the vapor–liquid phase diagram for this asymmetric Lennard–Jones mixture in bulk and in a hard slit-like pore with pore width $H = 10\sigma_{11}$. In this figure, the errors of the vapor–liquid coexistence are smaller than the size of the symbols. The system equilibrium pressures in the hard slit-like pore are higher than those in bulk, while the azeotropic composition changes very little by the confinement of hard wall. The observation that saturation pressure under the slit pore confinement is generally higher than

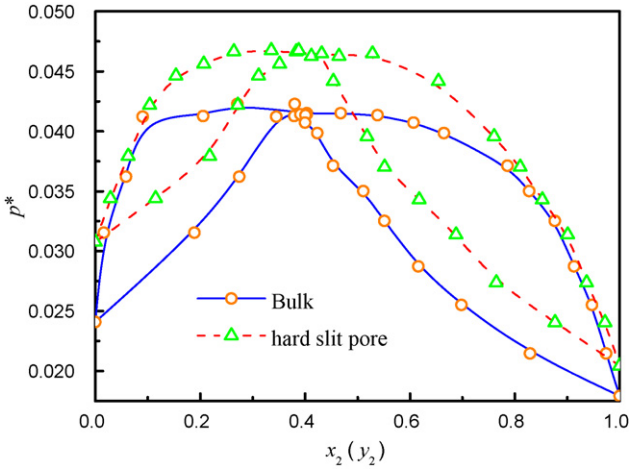

Fig. 3. Vapor–liquid phase diagram for the asymmetric Lennard–Jones mixture in bulk and in hard slit-like pore with pore width $H^* = 10.0$ at reduced temperature $T^* = 1.0$.

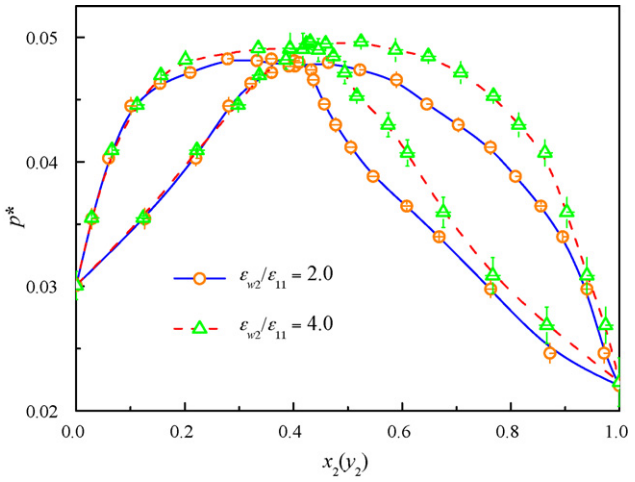

Fig. 4. Vapor–liquid phase diagram for the asymmetric Lennard–Jones mixture confined in slit-like pore with pore width $H/\sigma_{11} = 10.0$ and fluid–wall interaction parameters $\varepsilon_{w1}/\varepsilon_{11} = 2.0$, and $\varepsilon_{w2}/\varepsilon_{11} = 2.0$ and 4.0 at reduced temperature $T^* = 1.0$.

the bulk saturation ones is in accordance with that for the confined pure fluid [32].

The effect of the interaction strength between fluid and pore wall is investigated by fixing the interaction energy parameter between fluid component 1 and pore wall as $\varepsilon_{w1}/\varepsilon_{11} = 2.0$ and varying the interaction energy parameter between fluid component 2 and pore wall from $\varepsilon_{w2}/\varepsilon_{11} = 2$ to $\varepsilon_{w2}/\varepsilon_{11} = 20$. The pore width in these cases is $H = 10\sigma_{11}$, and the external potential is given by Eq. (3). Figs. 4–6 depict the vapor–liquid phase diagram for the asymmetric Lennard–Jones mixture confined in the slit-like pore at different ε_{w2}. In Figs. 4–6, $p* = p\sigma_{11}^3/\varepsilon_{11}$ is the reduced pressure, x_2 is the mole fraction of component 2 in liquid phase and y_2 is the mole fraction of component 2 in vapor phase. Table 2 gives the azeotropic compositions and pressures for the binary asymmetric Lennard–Jones mixture at different ε_{w2}. There is a small drop in azeotropic composition at $\varepsilon_{w2}/\varepsilon_{11} = 2$, as compared to that for the hard-wall pore. This drop is probably due to the statistical error in this case, and it does not mean any non-monotonic behavior. From Figs. 4–6 and Table 2 one can see that as the interaction strength ε_{w2} is increased, the azeotropic composition is shifted significantly towards component 2-rich side of the phase diagram and the azeotropic pressure increases greatly.

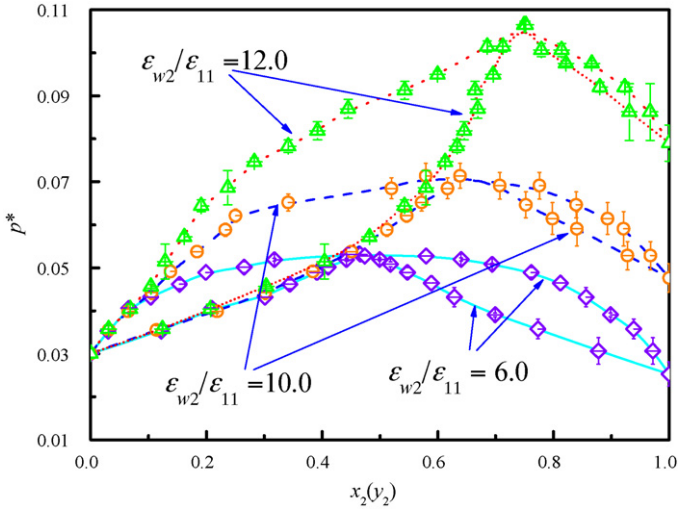

Fig. 5. Same as in Fig. 4 but for $\varepsilon_{w2}/\varepsilon_{11} = 6.0$, 10.0 and 12.0.

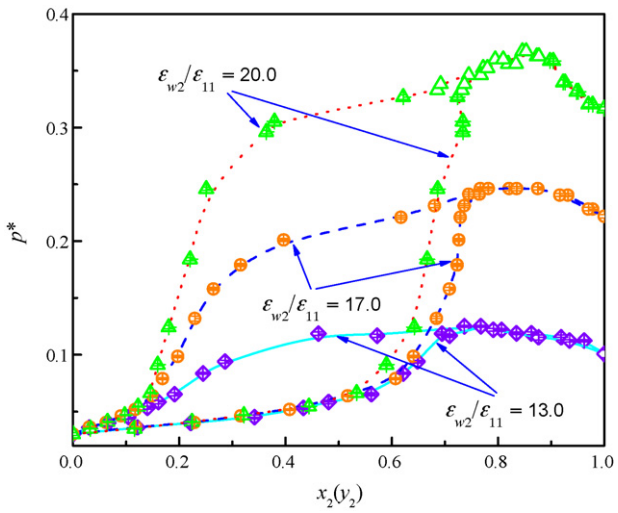

Fig. 6. Same as in Fig. 4 but for $\varepsilon_{w2}/\varepsilon_{11} = 13.0$, 17.0 and 20.0.

Qualitatively, it is easy to understand the phenomenon that the azeotropic composition for the binary asymmetric Lennard–Jones mixture changes significantly in the selective slit-like pores. Taking the short range side of the Lennard–Jones (9–3) potential into account, we may assume that in the region far from the wall, the

Table 2
Azeotropic compositions and pressures at various interaction strengths between fluid component 2 and the pore wall for the asymmetric Lennard–Jones fluid mixtures confined in the slit-like pores with pore width $H = 10\sigma_{11}$ and $\varepsilon_{w1} = 2.0\varepsilon_{11}$ at reduced temperature $T^* = 1.0$.

$\varepsilon_{w2}/\varepsilon_{11}$	x_2^{az}	p^{*az}
Bulk	0.390 ± 0.009	0.0416 ± 0.0004
Hard wall	0.400 ± 0.019	0.0466 ± 0.0002
2.0	0.397 ± 0.019	0.0479 ± 0.0002
4.0	0.420 ± 0.014	0.0495 ± 0.0002
6.0	0.468 ± 0.012	0.0529 ± 0.0005
8.0	0.546 ± 0.027	0.0583 ± 0.0004
10.0	0.648 ± 0.035	0.0651 ± 0.0005
12.0	0.750 ± 0.044	0.1042 ± 0.0007
13.0	0.787 ± 0.012	0.1145 ± 0.0014
14.0	0.832 ± 0.002	0.1441 ± 0.0014
16.0	0.851 ± 0.019	0.2033 ± 0.0040
17.0	0.874 ± 0.013	0.2440 ± 0.0039
20.0	0.917 ± 0.012	0.3464 ± 0.0094

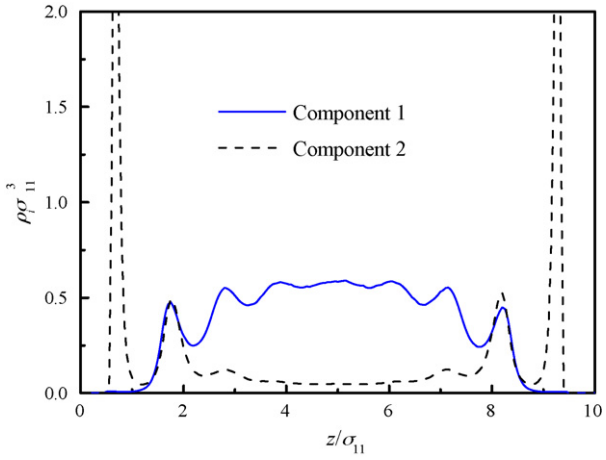

Fig. 7. The density profiles of the liquid phase for the binary asymmetric Lennard–Jones mixture in slit-like pores at reduced temperature $T^*=1.0$ when the total mole fraction of component 2 is 0.5. The slit-like pore parameters are $H/\sigma_{11}=10.0$, $\varepsilon_{w1}/\varepsilon_{11}=2.0$ and $\varepsilon_{w2}/\varepsilon_{11}=20.0$.

phase behavior is almost the same as that in bulk and therefore this partial azeotropic composition is the same as that in bulk. While in the region near the wall, due to the stronger adsorption field exerted by the wall on fluid component 2 than on fluid component 1, the densities of fluid component 2 are larger than that in bulk, while the densities of fluid component 1 are smaller than that in bulk, as can be seen from Fig. 7. This results in a larger mole fraction of fluid component 2 near the pore wall. Considering the contributions of two regions together, we obtained that the azeotropic composition of the system is shifted from bulk azeotropic point to component 2-rich side of the phase diagram.

It can be also seen from Fig. 7 that in the case of strong component 2–wall interaction ε_{w2} (e.g., $\varepsilon_{w2}/\varepsilon_{11}=20.0$), a greater amount of fluid component 2 accumulates at the first and second layers near the pore wall, while molecules of fluid component 1 are excluded from the first layer and stay at the second layer and the middle region of the pore.

Fig. 8 depicts the density-composition phase diagram for the asymmetric Lennard–Jones mixture in various external potentials. Here $\rho*=\left(\rho_1\sigma_{11}^3+\rho_2\sigma_{11}^3\right)$ is the total reduced density, ρ_1 and ρ_2 are the number densities of fluid components 1 and 2, respectively. Compared with Figs. 4–6, we can see that no matter whether in bulk or in the slit-like pores, the azeotropic point of the binary Lennard–Jones mixture locates at the compositions corresponding to the maximum of vapor density and the minimum of liquid density. In the slit-like pores with weak interactions between fluid and the pore wall, i.e., $\varepsilon_{w2}/\varepsilon_{11}$ ranges from 2.0 to 12.0 [see Fig. 8(a)], the increase of ε_{w2} causes considerable increases in the density of both coexisting phases in the entire range of composition, and larger increases are observed for vapor phase. What is interesting is that in the slit-like pores with ε_{w2} greater than 13.0 [see Fig. 8(b)], the density of liquid phase decreases with the increase of ε_{w2} near the azeotropic composition, around which some concave curves are observed. The stronger the adsorption field exerted by the wall on fluid component 2 is, the deeper the concave is.

Fig. 9 depicts the influence of the interaction strength between fluid component 2 and pore wall on the relative volatility for the binary asymmetric Lennard–Jones mixture confined in the slit-like pores at reduced temperature $T^*=1.0$. Here the relative volatility of component 2 with respect to component 1 is defined as

$$\alpha_{12}=\frac{\left(y_2/x_2\right)}{\left(y_1/x_1\right)} \tag{5}$$

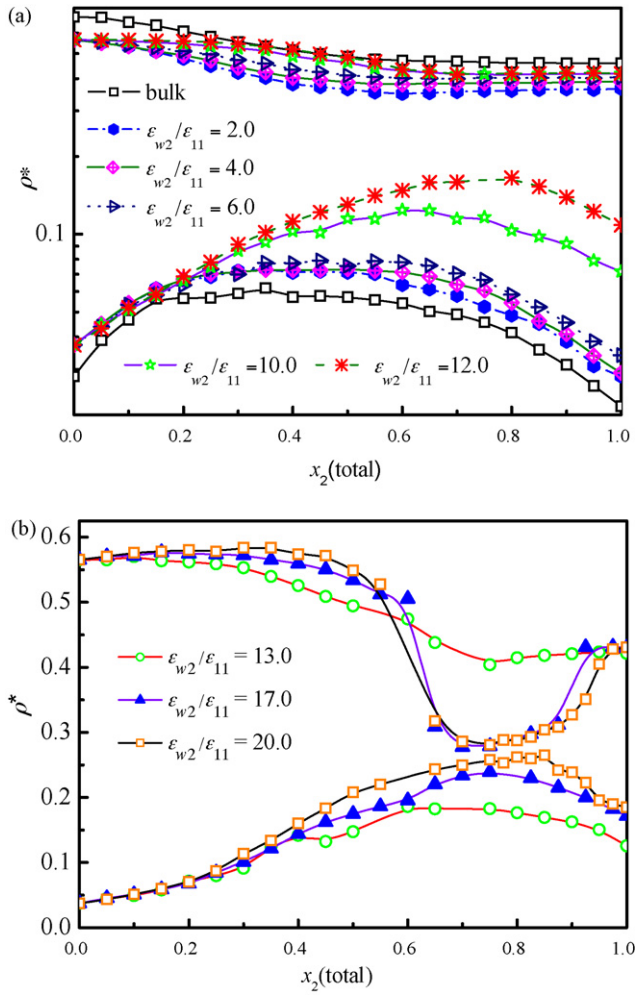

Fig. 8. Vapor–liquid coexisting densities for the binary asymmetry Lennard–Jones mixture at reduced temperature $T^*=1.0$ and confined in slit-like pores with pore with $H/\sigma_{11}=10.0$ and various fluid–wall interactions: $\varepsilon_{w1}/\varepsilon_{11}=2.0$ and $\varepsilon_{w2}/\varepsilon_{11}=2.0$, 4.0, 6.0, 10.0, 12.0, 13.0, 17.0 and 20.0.

The relative volatility $\alpha_{12}=1.0$ corresponds to the azeotropic point.

From Fig. 9 we can see that in the slit-like pore with the interactions $\varepsilon_{w1}/\varepsilon_{11}=\varepsilon_{w2}/\varepsilon_{11}=2.0$, the azeotropic composition and the relative volatilities at $x_2>0.2$ are almost the same as those in bulk. As the interaction strength between component 2 and the pore wall becomes stronger, the azeotropic composition is shifted towards the increase of the mole fraction of fluid component 2, and the relative volatility increases simultaneously. When the interaction strength ε_{w2} is large enough, there is a peak on the curve of relative volatility as a function of mole fraction of fluid component 2, and the relative volatility is close to unity when the mole fraction of fluid component 2 is larger than the azeotropic composition. This phenomenon corresponds to the overlap of the liquid and vapor branches when x_2 is larger than the azeotropic composition for $\varepsilon_{w2}\geq 12.0$.

To explore the dependence of the vapor–liquid phase equilibria of the binary asymmetric Lennard–Jones mixture on the pore width, simulations were carried out in the slit-like pores with the fluid–wall interactions $\varepsilon_{w1}/\varepsilon_{11}=\varepsilon_{w2}/\varepsilon_{11}=2.0$ and pore widths $H/\sigma_{11}=4.5$, 6, 7.5 and 10. The obtained pressure-composition phase diagram is presented in Fig. 10, and the azeotropic compositions and pressures are summarized in Table 3. It is observed from Table 3 that the azeotropic compositions are nearly unchanged with the variation in the pore width, and are

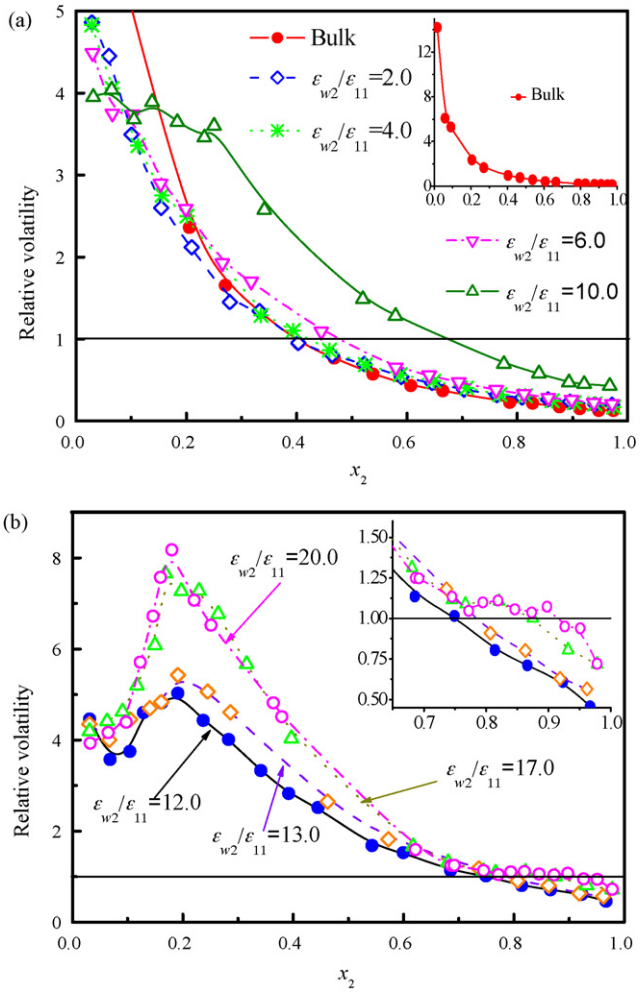

Fig. 9. Relative volatility for the binary asymmetric Lennard–Jones mixture at reduced temperature T^* = 1.0 and confined in slit-like pores with pore width $H = 10\sigma_{11}$, and fluid–wall interactions $\varepsilon_{w1}/\varepsilon_{11} = 2.0$ and $\varepsilon_{w2}/\varepsilon_{11} = 2.0$, 4.0, 6.0, 10.0, 12.0, 13.0, 17.0 and 20.0.

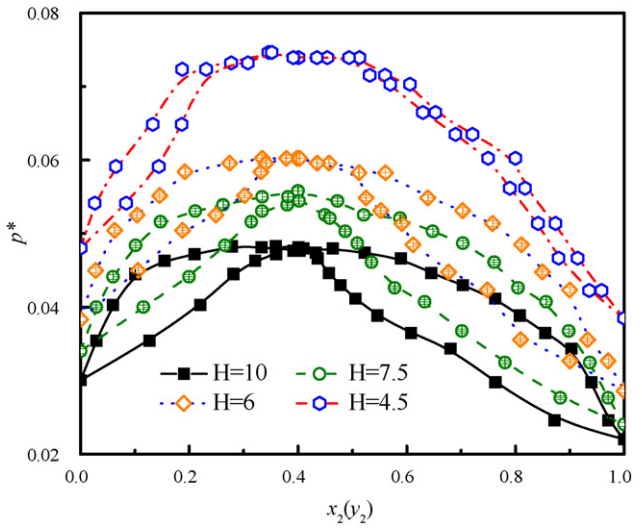

Fig. 10. Vapor–liquid phase diagrams for the binary asymmetric Lennard–Jones mixture confined in the slit-like pores with the fluid–wall interactions $\varepsilon_{w1}/\varepsilon_{11} = \varepsilon_{w2}/\varepsilon_{11} = 2.0$ and pore widths H/σ_{11} = 4.5, 6.0, 7.5 and 10.0 at reduced temperature T^* = 1.0. The errors are smaller than the symbol size.

Table 3
Azeotropic compositions and pressures for the asymmetry Lennard–Jones fluid mixtures confined in the slit-like pores with different widths at reduced temperature T^* = 1.0. The fluid–pore wall interaction energy parameters are $\varepsilon_{w1} = \varepsilon_{w2} = 2.0\varepsilon_{11}$.

H^*	x_2^{az}	p^{*az}
10.0	0.397 ± 0.019	0.0479 ± 0.0002
7.5	0.397 ± 0.009	0.0555 ± 0.0006
6.0	0.401 ± 0.012	0.0603 ± 0.0001
4.5	0.383 ± 0.034	0.0744 ± 0.0003

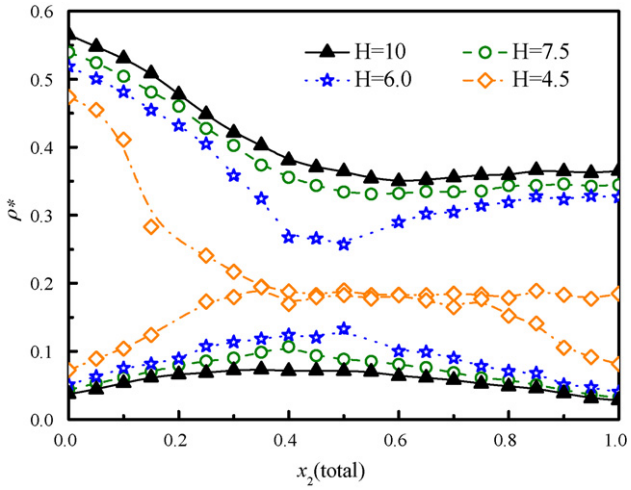

Fig. 11. Vapor–liquid coexisting densities for the binary asymmetry Lennard–Jones mixture confined in the slit-like pores with various widths H/σ_1 = 4.5, 6.0, 7.5 and 10.0 at reduced temperature T^* = 1.0. The fluid–wall interaction energy parameters are $\varepsilon_{w1}/\varepsilon_{11} = \varepsilon_{w2}/\varepsilon_{11} = 2.0$.

almost the same as that in bulk. There should not be any non-monotonic behavior of azeotropic composition as a function of pore size. The small value of azeotropic composition for the pore width $H/\sigma_{11} = 4.5$ is due to large statistical error because in this case the vapor–liquid two phase region is very narrow in the phase diagram, leading to great difficulty in determining which point is azeotrope [see Fig. 10]. This can be judged from the information on the errors given in Table 3. The azeotropic pressure, however, increases significantly as the pore becomes narrower. The area of the vapor–liquid region becomes smaller as the pore width is

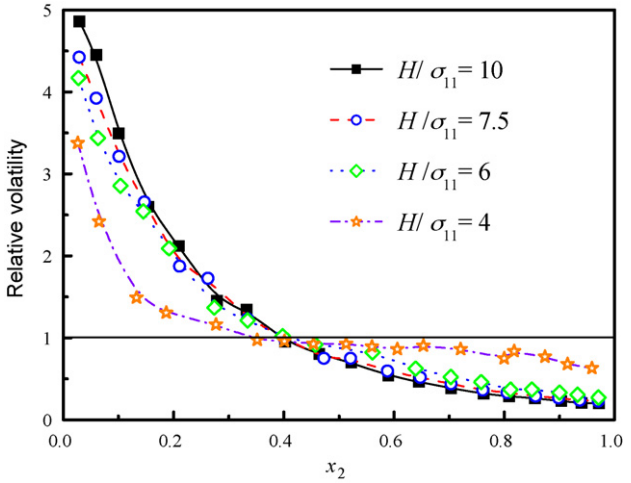

Fig. 12. Relative volatility for the asymmetric Lennard–Jones mixture confined in slit-like pores with various widths H/σ_{11} = 4.5, 6.0, 7.5 and 10.0 at reduced temperature T^* = 1.0. The fluid–wall interaction energy parameters are $\varepsilon_{w1}/\varepsilon_{11} = \varepsilon_{w2}/\varepsilon_{11} = 2.0$.

decreased. Fig. 11 depicts the density-composition phase diagram for the binary asymmetric Lennard–Jones mixture confined in the slit-like pore with different widths. The liquid density decreases while the vapor density increases as the pore width becomes narrower. Fig. 12 depicts the relative volatility for the binary mixture confined in the slit-like pore with different pore widths. It is shown that when the pore becomes narrower, the relative volatility is much closer to unity, indicating that the phase selectivity for the binary mixture decreases in the whole range of composition.

4. Conclusions

We have performed the GEMC simulation for the binary symmetric Lennard–Jones mixture in bulk and square-well fluid in the slit pore. The simulated results have been compared with the previous work in order to validate our GEMC simulation program. After that, we have studied the effect of the pore width and fluid–wall interaction on the vapor–liquid phase equilibrium, azeotropic composition and pressure as well as the relative volatility for the binary asymmetric Lennard–Jones mixture confined in the slit-like pores.

For the binary asymmetric Lennard–Jones mixture, when the pore width and the interaction strength between fluid component 1 and pore wall are fixed and as the interaction strength between component 2 and the pore wall is increased, the azeotropic point of the system is shifted from $x_2 = 0.390$ to 0.917, and the azeotropic pressure increases considerably. The azeotropic point locates at the composition corresponding to the maximum of vapor density and the minimum of liquid density. With the increase of fluid component 2–wall interaction ε_{w2}, the relative volatility increases. In the unselective slit-like pores, the azeotropic composition for the binary asymmetric Lennard–Jones mixture is nearly unchanged with the variation in pore width. The liquid density decreases while the vapor density increases as the pore becomes narrower. The phase selectivity decreases with the narrowing of the slit-like pore in the whole range of composition.

All the simulated results indicate that the azeotropic composition can be shifted or even be removed by the confinement. The selectivity of vapor–liquid phase equilibrium can be influenced greatly by changing the pore width or fluid–pore wall interaction. From all the results obtained in the simulations we may conclude that the confinement can provide a new way to separate the binary mixtures with azeotropic points.

Acknowledgments

We would like to make an acknowledgment to Yong-Jun Du for her effort in preparing the manuscript. This work is supported by National Natural Science Foundation of China (no. 20876083 and no. 20736003), Specialized Research Fund for the Doctoral Program of Higher Education (no. 20070003099) and the Program for New Century Excellent Talents in University (NCET) of China.

References

[1] J. Puibasset, Adsorption/desorption hysteresis of simple fluids confined in realistic heterogeneous silica mesopores of micrometric length: a new analysis exploiting a multiscale Monte Carlo approach, J. Chem. Phys. 127 (2007) 154701.
[2] W.R. Smit, H.L. Vortler, Monte Carlo simulation of fluid phase equilibria in pore systems: square-well fluid distributed over a bulk and a slit-pore, Chem. Phys. Lett. 249 (1996) 470–475.
[3] G.J. Zarragoicoechea, V.A. Kuz, Critical shift of a confined fluid in a nanopore, Fluid Phase Equilib. 220 (2004) 7–9.
[4] A. Vishnyakov, E.M. Piotrovskaya, E.N. Brodskaya, E.V. Votyakov, Y.K. Tovbin, Critical properties of Lennard–Jones fluids in narrow slit-shaped pores, Langmuir 17 (2001) 4451–4458.
[5] B. Peng, Y.-X. Yu, A density functional theory with a mean-field weight function: applications to surface tension, adsorption, and phase transition of a Lennard–Jones fluid in a slit-like pore, J. Phys. Chem. B 112 (2008) 15407–15416.
[6] T. Miyata, A. Endo, T. Yamamoto, T. Ohmor, T. Akiya, M. Nakaiwa, Gibbs ensemble Monte Carlo simulation of LJ fluid in cylindrical pore with energetically heterogeneous surface, Mol. Phys. 30 (2004) 353–359.
[7] M. Schoen, C.L. Rhykerd Jr., J.H. Cushman, D.J. Diestler, Slit-pore sorption isotherms by the grand-canonical Monte Carlo method—manifestations of hysteresis, Mol. Phys. 66 (1989) 1171–1182.
[8] Y.-X. Yu, F.-Q. You, Y.P. Tang, G.H. Gao, Y.-G. Li, Structure and adsorption of a hard-core multi-Yukawa fluid confined in a slitlike pore: grand canonical Monte Carlo simulation and density functional study, J. Phys. Chem. B 110 (2006) 334–341.
[9] B. Coasne, R. Pellenq, A grand canonical Monte Carlo study of capillary condensation in mesoporous media: effect of the pore morphology and topology, J. Chem. Phys. 121 (2004) 3767–3774.
[10] D.D. Do, H.D. Do, Effects of potential models in the vapor–liquid equilibria and adsorption of simple gases on graphitized thermal carbon black, Fluid Phase Equilib. 236 (2005) 169–177.
[11] M. Aoshima, T. Suzuki, K. Kaneko, Molecular association-mediated micropore filling of supercritical Xe in a graphite slit pore by grand canonical Monte Carlo simulation, Chem. Phys. Lett. 310 (1999) 1–7.
[12] Y.-X. Yu, A novel weighted density functional theory for adsorption, fluid-solid interfacial tension, and disjoining properties of simple liquid films on planar solid surfaces, J. Chem. Phys. 131 (2009) 024704.
[13] B. Peng, Y.-X. Yu, A density functional theory for Lennard–Jones fluids in cylindrical pores and its applications to adsorption of nitrogen on MCM-41 materials, Langmuir 24 (2008) 12431–12439.
[14] A.Z. Panagiotopoulos, N. Quirke, M. Stapleton, D.J. Tildesley, Phase-equilibria by simulation in the Gibbs ensemble—alternative derivation, generalization and application to mixture and membrane equilibria, Mol. Phys. 63 (1988) 527–545.
[15] D.A. Kofke, E.D. Glandt, Monte-Carlo simulation of multicomponent equilibria in a semigrand canonical ensemble, Mol. Phys. 64 (1988) 1105–1131.
[16] D.A. Kofke, Gibbs–Duhem integration—a new method for direct evaluation of phase coexistence by molecular simulation, Mol. Phys. 78 (1993) 1331–1336.
[17] V.K. Shen, J.R. Errington, Determination of fluid-phase behavior using transition-matrix Monte Carlo: binary Lennard–Jones mixtures, J. Chem. Phys. 122 (2005) 064508.
[18] S.C. McGrother, K.E. Gubbins, Constant pressure Gibbs ensemble Monte Carlo simulations of adsorption into narrow pores, Mol. Phys. 97 (1999) 955–965.
[19] M. Kettler, H.L. Vortler, I. Nezbeda, M. Strnad, Coexistence properties of higher n-alkanes modelled as Kihara fluids: Gibbs ensemble simulations, Fluid Phase Equilib. 181 (2001) 83–94.
[20] J. Carrero-Mantilla, M. Llano-Restrepo, Vapor–liquid equilibria of the binary mixtures nitrogen plus methane, nitrogen plus ethane and nitrogen plus carbon dioxide, and the ternary mixture nitrogen plus methane plus ethane from Gibbs-ensemble molecular simulation, Fluid Phase Equilib. 208 (2003) 155–169.
[21] A.Z Panagiotopoulos, Adsorption and capillary condensation of fluids in cylindrical pores by Monte Carlo simulation in the Gibbs ensemble, Mol. Phys. 62 (1987) 701–719.
[22] E. Kierlik, Y. Fan, P.A. Monson, M.L. Rosinberg, Liquid–liquid equilibria in a slit pore: Monte Carlo simulation and mean field density functional theory, J. Chem. Phys. 102 (1995) 3712–3719.
[23] W.T. Gozdz, K.E. Gubbins, A.Z. Panagiotopoulos, Liquid–liquid phase transitions in pores, Mol. Phys. 84 (1995) 825–834.
[24] M. Sliwinska-Bartkowiak, R. Sikorski, S.L. Sowers, L.D. Gelb, K.E. Gubbins, Phase separations for mixtures in well-characterized porous materials: liquid–liquid transitions, Fluid Phase Equilib. 136 (1997) 93–109.
[25] H. Kanda, H. Makino, Liquid–liquid phase separation of binary Lennard–Jones fluid in slit nanopores, Adsorption 14 (2008) 485–491.
[26] G. Morrison, M.O. McLinden, Azeotropy in refrigerant mixtures, Rev. Int. Froid 16 (1993) 129–138.
[27] M. Cismoudi, M.L. Michelsen, M.S. Zabaloy, Automated generation of phase diagrams for binary systems with azeoptropic behavior, Ind. Eng. Chem. Res. 47 (2008) 9728–9743.
[28] V.I. Harismiadis, J. Vorholz, A.Z. Panagiotopoulos, Efficient pressure estimation in molecuar simulations without evaluating the virial, J. Chem. Phys. 105 (1996) 8469–8470.
[29] H.L. Vortler, W.R. Smith, Computer simulation studies of a square-well fluid in a slit pore. Spreading pressure and vapor–liquid phase equilibria using the virtual-parameter-variation method, J. Chem. Phys. 112 (2000) 5168–5174.
[30] H. Flyvbjerg, H.G. Petersen, Errors estimates on averages of correlated data, J. Chem. Phys. 91 (1989) 461–466.
[31] M. Mehta, D.A. Kofke, Coexistence diagrams of mixtures by molecular simulation, Chem. Eng. Sci. 49 (1994) 2633–2645.
[32] J.K. Singh, S.K. Kwak, Surface tension and vapor–liquid phase coexistence of confined square-well fluid, J. Chem. Phys. 126 (2007) 024702.